ISSN 1990-7931, Russian Journal of Physical Chemistry B, 2019, Vol. 13, No. 1, pp. 86–95. © Pleiades Publishing, Ltd., 2019.
Russian Text © G.N. Muradyan, S.K. Dolukhanyan, A.G. Aleksanyan, O.P. Ter-Galstyan, N.L. Mnatsakanyan, 2019, published in Khimicheskaya Fizika, 2019, Vol. 38, No. 1, pp. 38–48.

COMBUSTION, EXPLOSION, AND SHOCK WAVES

Regularities and Mechanism of Formation of Aluminides in the TiH_2–ZrH_2–Al System

G. N. Muradyan[a], S. K. Dolukhanyan[a, *], A. G. Aleksanyan[a], O. P. Ter-Galstyan[a], and N. L. Mnatsakanyan[a]

[a] *Nalbandyan Institute of Chemical Physics, National Academy of Sciences of Armenia, Yerevan, 0014 Armenia*

**e-mail: seda@ichph.sci.am*

Received March 21, 2018; revised May 25, 2018; accepted June 20, 2018

Abstract—The results of our study of the formation of aluminides in the Ti–Al–Zr system by the hydride cycle (HC) method were presented. The characteristics of aluminides (phase composition, density, and absorption properties) were found to depend on the ratios of titanium and zirconium hydrides and aluminum powders, pressure during compaction of the reaction mixture, and dehydrogenation and sintering modes. A series of single- and double-phase aluminides based on titanium and zirconium were synthesized. Some of the synthesized aluminides reacted with hydrogen without preliminary grinding in the self-propagating high-temperature synthesis (SHS) mode, forming reversible hydrides. The concentration triangle of the Ti–Al–Zr system was constructed. The HC method for the synthesis of aluminides based on titanium and zirconium has significant advantages over the conventional techniques: relatively low temperatures (no more than 1000°C); reaction time ~30–60 min; one-stage formation of single-phase aluminides. The single-phase aluminides $Ti_{0.25}Al_{0.75}$, $Zr_{0.25}Al_{0.75}$, $Ti_{0.05}Zr_{0.2}Al_{0.75}$, and others were synthesized at temperatures of 650–670°C.

Keywords: hydride cycle (HC) method, self-propagating high-temperature synthesis (SHS), titanium–zirconium aluminides, metal hydrides, hydrogenation–dehydrogenation, intermetallic compounds, alloys of refractory metals

DOI: 10.1134/S199079311901010X

INTRODUCTION

The goal of the present study was to investigate the formation of titanium and zirconium aluminides by the hydride cycle (HC) method. Aluminum-based alloys have a number of characteristics that make them especially attractive in modern technology. As is known, aluminum alloys are highly resistant to oxidation due to the extremely stable passivating protective oxide layer. Aluminides are characterized by low density, high strength, heat resistance, and other properties. Aluminum alloys are much more economical than the existing high-temperature alloys based on Ni and Ti. Therefore, interest in aluminum-based alloys is associated with their numerous and important practical applications as structural materials: in defense industry; in aerospace, atomic, and hydrogen energy; shipbuilding, chemical, automobile, and other sectors of transport engineering; machine tool industry; metalworking industry; radio engineering; electronics; electric engineering; medicine (biocompatible materials), etc.

Many works were devoted to the methods for the synthesis of aluminides and their properties. The review by L. Tretyachenko on the aluminum–titanium–zirconium system covering 1961–2003 gave references to 44 articles. Many new publications have appeared on the synthesis and studies of these materials due to the increasing interest in aluminides.

The well-known methods for the synthesis of aluminides are induction and arc melting, which require sophisticated equipment (high-temperature or arc furnaces) [2–6]. In powder metallurgy, aluminides are synthesized by thermal treatment of the reaction mixture at $T = 850$–900°C for more than 40 h [7]. In the mechanochemical method, the reaction mixture sticks to the drum wall when stirred in drums for more than 60 h, which leads to a change in the ratio of components and contamination of the products with ball and drum materials [8].

The differences in the density or melting and evaporation temperature of the batch components (for example, Al–Ti, Al–Zr, etc.) complicate modern technologies. The dense oxide film on the particle surface of metal powders prevents the mutual diffusion of the components. These methods for the synthesis of aluminides are prolonged and multistage and require multiple remelting, high vacuum, and inert medium at high temperatures (1600–2500°C). In recent decades, aluminides were synthesized by self-propagating high-temperature synthesis (SHS). Its implementation,

however, often requires additional activation of the initial batch. Therefore, the search for new ways for the synthesis of aluminides of the given composition and structure is evidently a challenge in modern materials science.

Here we used the hydride cycle method developed at the Institute of Chemical Physics, National Academy of Sciences of Armenia, to synthesize aluminides of refractory metals. The method consists in the use of hydrides of refractory metal as the starting materials for the synthesis of alloys or metal hydrides and another metal (Ni, Co, Al, etc.). The HC method and the experimental data obtained in the syntheses of alloys and intermetallic compounds based on refractory metals were described in detail in [9–16]. The HC method in combination with SHS allowed us to develop effective processes for the formation of various binary and multicomponent alloys and intermetallic compounds and to synthesize their hydrides.

EXPERIMENTAL

Titanium hydride (TiH_2, 4.01 wt % H_2) and zirconium hydride (ZrH_2, 2 wt % H_2) were preliminarily synthesized by SHS [17]. The resulting hydrides were ground to a fraction of <50 μm and thoroughly mixed with aluminum powder (99.7% purity). For the synthesis of hydrides, zirconium (99.9% (PTsRK) and titanium (PTM-1) were used. The TiH_2 and ZrH_2 powders are so brittle that during the preparation of the reaction mixture $xTiH_2 + yZrH_2 + zAl \rightarrow Ti_xAl_zZr_y$ for 30–40 min, the hydrides continued to granulate to a fraction of less than 10 μm. It should be noted that the starting hydrides have nanosized crystallite particles of less than 50 nm [18].

The reaction mixture was pressed in a collet mold into cylindrical tablets with a diameter of $d = 22$ mm and a height of $h = 15–25$ mm on a hydraulic press (at a pressing force from 20000 to 45000 kgf). The HC process was performed in sealed quartz reactors equipped with a stove and devices for vacuum and temperature control. The sample was heated to 1000°C.

The samples were identified by chemical, differential-thermal (DTA, Q-1500 derivatograph), and X-ray diffraction (XRD, DRON-0.5 diffractometers) analyses. The first analysis (DTA) was performed by heating the sample to 1000°C at a rate of 20°C/min. The sample density was measured by the hydrostatic method; the X-ray density was calculated from crystal lattice parameters. The density of the obtained samples was measured for pellets pressed at a pressing pressure of $P = 30000$ kgf.

We studied the influence of the ratios of titanium and zirconium hydrides and aluminum powders, pressure during compaction of the reaction mixture, and dehydrogenation and sintering modes (temperature and heating rate) on the characteristics of aluminides (phase composition, density, and absorption properties). Below are the results obtained in a study of the following three compositions.

1. $(0.75 - x)TiH_2$–$xZrH_2$–0.25Al System (Ti_3Al–Zr_3Al section, 25 at % Al)

The $Ti_{0.75-x}Al_{0.3}Zr_x$ pseudo-binary composite prepared by arc melting in pure argon was studied in [4]. It was shown that hydrogenation at room temperature and up to 473 K leads to the formation of amorphous aluminide hydride with an H/Me ratio of 1.10. The stability of the Ti_2ZrAl phase was considered and the preferred positions of Zr atoms in Ti_3Al were shown in [19]. An isothermal section of the Al–Ti–Zr ternary system at 1073 K was constructed in [2] by analyzing the ternary diffusion and equilibrium alloys on an electron probe microanalyzer (electron probe microanalysis EPMA).

Earlier, our studies of the formation of bimetallic aluminides Ti_3Al and Zr_3Al in a HC revealed some differences in the mechanism of their formation [13, 15].

The system with two transition metal hydrides $(0.75 - x)TiH_2$–$xZrH_2$–0.25Al studied in this work is more complex. Below is the reaction of formation of aluminides based on titanium and zirconium in the HC mode: $(0.75 - x)TiH_2 + xZrH_2 + 0.25Al \rightarrow Ti_{0.75-x}Al_{0.25}Zr_x + H_2\uparrow$, where $0 \le x \le 0.75$.

Figure 1a shows an HC thermogram of the $Ti_{0.55}Al_{0.25}Zr_{0.2}$ composite. All the HC thermograms showed exothermal peaks at 650–670°C when the initial $(0.75 - x)TiH_2 + xZrH_2 + 0.25Al$ batch was heated, which indicated that aluminum reacted with titanium and zirconium formed as a result of the dissociation of the corresponding hydrides.

Table 1 gives the characteristics of aluminides synthesized in HC in the $(0.75 - x)TiH_2$–$xZrH_2$–0.25Al system. For comparison, the table also shows the characteristics of binary aluminides Ti_3Al and Zr_3Al. According to X-ray diffraction data, the reaction products are the solid solutions of the B_2 and (α_2) $D0_{19}$ phases depending on the ratio of the titanium and zirconium hydride contents. At 15 at % TiH_2 in the starting batch, the B_2 phase appears among the reaction products along with the solid solution of Al and Ti in Zr. As the TiH_2 content increases, the content of B_2 also increases, it becomes the main phase, and the α_2 phase ($D0_{19}$) appears. At 65 at % TiH_2, the dominant phase is the hexagonal $D0_{19}$, whose lattice parameters are close to those of the hexagonal phase of titanium aluminide α_2-Ti_3Al.

To evaluate the thermal effects during the heating of the ($0.55TiH_2 + 0.2ZrH_2 + 0.25Al$) batch to 1000°C, a differential thermal analysis was performed (Fig. 1b). The DTA curve (*2*, Fig. 1b) has three pronounced endo effects: at 150, 520, and 640°C, which are due to the decomposition of the starting hydrides

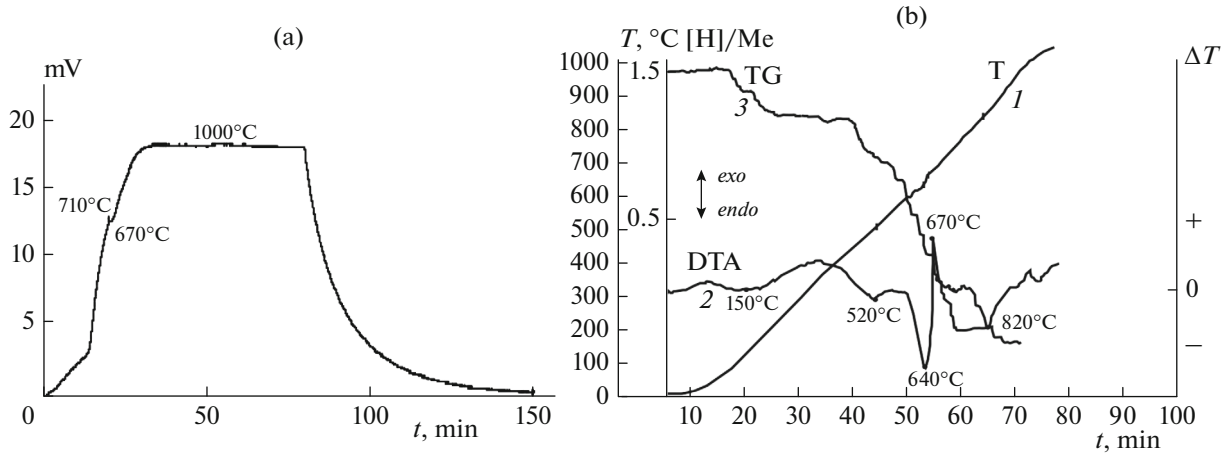

Fig. 1. (a) Thermogram of formation of aluminide $Ti_{0.55}Al_{0.25}Zr_{0.2}$ in HC; (b) DTA curves during the heating of the $0.55TiH_2 + 0.20ZrH_2 + 0.25Al$ batch.

TiH_2 and (partially) ZrH_2. According to Fig. 1b, the exothermal peak observed at 670°C on curve *2* coincides well with the exo peak observed on the HC thermogram (Fig. 1a) and suggests that an exothermal reaction occurred between the decomposition products of titanium and zirconium hydrides and aluminum. According to the XRD data, intermediate products quenched at 670°C are complex alumohydrides based on titanium and zirconium. The fourth endo effect at 820°C is caused by the decomposition of the intermediate alumohydride. According to the XRD data, the final reaction product ($0.55TiH_2 + 0.2ZrH_2 + 0.25Al$) in HC and after DTA is two-phase aluminide $Ti_{0.55}Al_{0.25}Zr_{0.2}$ (B_2 phase; $a = 3.318 + (\alpha_2)\,D0_{19}$). When the starting $(0.75 - x)TiH_2 + xZrH_2 + 0.25Al$ batch was heated (Table 1), all the DTA curves showed similar patterns when the temperature increased to 1000°C, except that the intensity of the exo and endo effects changed depending on the TiH_2/ZrH_2 ratio.

Table 1. Characteristics of aluminides in the $(0.75–x)TiH_2–xZrH_2–0.25Al$ system synthesized by HC

Starting reagents, at %			Phase composition; lattice parameters, Å	Calculated formula	T_{comb}, °C	H_2, wt %	Formula of aluminide hydride, type of crystal lattice	Density, g/cm^3 (hydrostat.)
TiH_2	Al	ZrH_2						
0	25	75	sol. soln., Al in the Zr + X HCP phase; $a = 3.242$, $c = 5.176$	$Zr_{0.75}Al_{0.25}$	540	1.47	$Zr_{0.75}Al_{0.25}H_{1.07}$; BCT + X phase	5.864
15	25	60	sol. soln. of Al and Ti in Zr; $a = 3.234$, $c = 5.178$+ B_2 phase	$Ti_{0.15}Al_{0.25}Zr_{0.6}$	430	1.3	$Ti_{0.15}Zr_{0.6}Al_{0.25}H_{0.89}$	5.221
25	25	50	sol. soln. of Al and Ti in Zr; $a = 3.243$, $c = 5.175$ + B_2 phase	$Ti_{0.25}Zr_{0.5}Al_{0.25}$	430	1.3	$Ti_{0.25}Zr_{0.5}Al_{0.25}H_{0.83}$	5.193
35	25	40	B_2 phase; $a = 3.384$ + sol. soln. of Al and Ti in Zr	$Ti_{0.35}Zr_{0.4}Al_{0.25}$	360	1.32	$Ti_{0.35}Zr_{0.4}Al_{0.25}H_{0.79}$	4.61
45	25	30	B_2 phase; $a = 3.348 + (\alpha_2)\ D0_{19}$	$Ti_{0.45}Zr_{0.3}Al_{0.25}$	330	1.57	$Ti_{0.45}Zr_{0.3}Al_{0.25}H_{0.87}$	4.429
55	25	20	B_2 phase; $a = 3.318 + (\alpha_2)\ D0_{19}$	$Ti_{0.55}Zr_{0.2}Al_{0.25}$	310	1.32	$Ti_{0.55}Zr_{0.2}Al_{0.25}H_{0.67}$	4.199
65	25	10	α_2-Ti_3Al ($D0_{19}$); $a = 5.894$, $c = 4.629$ + B_2 phase; $a = 3.307$	$Ti_{0.65}Zr_{0.1}Al_{0.25}$	300	1.28	$Ti_{0.65}Zr_{0.1}Al_{0.25}H_{0.59}$	4.134
75	25	0	α_2-Ti_3Al ($D0_{19}$); $a = 5.83$, $c = 4.647$	$Ti_{0.75}Al_{0.25}$	500	2.27	$Ti_{0.7}Al_{0.3}H_{1.0}$ fcc	3.457

Table 2. Characteristics of titanium and zirconium aluminides synthesized in HC in the $xTiH_2$–$(1-x)ZrH_2$–Al system (TiAl–ZrAl section, 50 at % Al)

Starting reagents, at %			Phase composition; lattice parameters, Å	Calculated formula	T_{comb}, °C (SHS)	H_2, wt %	Density, g/cm^3 (hydrostat.)
TiH_2	Al	ZrH_2					
0	50	50	Al_2Zr (hex.); $a = 5.293$, $c = 8.737$ + Zr + ZrAl (traces)	ZrAl	405	0.81	4.630
10	50	40	Al_2Zr; $a = 5.271$, $c = 8.892$ + Zr	$Ti_{0.1}Zr_{0.4}Al_{0.5}$	220	0.57	4.572
20	50	30	Al_2Zr; $a = 5.312$, $c = 8.556$+ + γ-TiAl (tetragonal)	$Ti_{0.2}Zr_{0.3}Al_{0.5}$	125	0.48	4.342
25	50	25	Al_2Zr; $a = 5.305$, $c = 8.755$ + γ-TiAl;	$Ti_{0.25}Zr_{0.25}Al_{0.5}$	188	0.45	4.167
30	50	20	Al_2Zr; $a = 5.299$, $c = 8.746$ + γ-TiAl; $a = 4.008$, $c = 4.096$	$Ti_{0.3}Zr_{0.2}Al_{0.5}$	160	0.42	4.036
40	50	10	γ-TiAl; $a = 4.014$, $c = 4.084$ + Al_2Zr; $a = 5.279$, $c = 8.746$	$Ti_{0.4}Zr_{0.1}Al_{0.5}$	–	–	3.031
47	47	6	γ-TiAl; $a = 4.001$, $c = 4.077$; Al_2Zr; $a = 5.277$, $c = 8.738$	$Ti_{0.47}Zr_{0.06}Al_{0.47}$	–	–	2.886
50	48	2	γ-TiAl; $a = 4.003$, $c = 4.076$ + X phase	$Ti_{0.5}Zr_{0.02}Al_{0.48}$	–	–	2.805
50	50	0	γ-TiAl; $a = 3.981$, $c = 4.051$	TiAl	–	–	2.75

To determine the absorption properties of the synthesized aluminides with respect to hydrogen and the hydrogen effect on the phase composition, the obtained compact aluminide pellets were burnt without prior crushing in hydrogen, at $P_H = 10$ atm. As a result of combustion ($T_c = 300$–430°C), aluminide hydrides containing hydrogen (H/Me ≥ 1.3–1.65) were synthesized (Table 1). All the hydrides are reversible: for example, $Ti_{0.375}Al_{0.25}Zr_{0.375} + H_2 \leftrightarrow Ti_{0.375}Al_{0.25}Zr_{0.375}H_{0.99}$.

2. $xTiH_2$–$(1-x)ZrH_2$–Al System (TiAl–ZrAl section, 50 at. % Al)

A series of Ti–Al–Zr ternary alloys with different compositions around the binary γ-TiAl ($L1_0$) were synthesized and annealed at 1273 K for 10 h with subsequent quenching [3]. The almost single-phase γ phase was obtained in a fairly wide range of compositions $Al_{50}(Ti_{50-x-y}Al_xZr_y)$ at $0 \le x \le 15$ and $0 \le y \le 15$. The lattice parameters **a** and **c** increase with the Zr concentration. The arc melting followed by homogenization at 1100°C for 100 h, heat treatment at 800°C + 600°C (for 3 h at each temperature), and air cooling to 25°C gave the single-phase aluminide γ phase 2Zr–50Ti–48Al (at %), as reported in [20]. The solubility limit of Zr in γ-TiAl was established, which was ~11 at % [21]. Earlier, we synthesized the single-phase aluminide γ-TiAl by the HC method [13]; it was shown that the single-phase ZrAl did not form in HC [15].

This section presents the results of studies of the reaction of formation of titanium and zirconium aluminides in the HC mode $xTiH_2 + (1-x)ZrH_2 + Al \rightarrow Ti_xAl\,Zr_{1-x} + H_2\uparrow$, where $0 \le x \le 1$. Table 2 shows the characteristics of aluminides obtained in HC at different ratios of the starting components (Ti_xAlZr_{1-x} series); for comparison, the characteristics of binary aluminides TiAl and ZrAl are also presented. A series of two-phase aluminides based on Ti, Al, and Zr of different compositions were obtained along with the γ-TiAl binary phase ($L1_0$). All the exo effects recorded on the thermograms and DTA curves are within 530–670°C.

3. $x(TiH_2)$–$(1-x)(ZrH_2)$–3Al System ($TiAl_3$–$ZrAl_3$ section, 75 at % Al)

The Group 4 (Ti, Zr, Hf) and 5 (V, Nb, Ta) metal trialuminides crystallize with a body-centered tetragonal structure $D0_{22}$ (for Al_3Ti) or $D0_{23}$ (for Al_3Zr). As is known, the high-temperature trialuminides used as structural materials have high strength; this primarily concerns Al_3Ti as it has the lowest density in this class.

However, the low-symmetry tetragonal structure makes these phases brittle. The $D0_{22}$ and $D0_{23}$ structures are closely related to the $L1_2$ cubic structure. Today, efforts are focused on doping these binary intermetallic compounds to transform them into the $L1_2$ structures of higher symmetry in the hope that an increase in the number of independent glide systems will improve the impact strength. For example, Al_3Ti ($D0_{22}$) can be transformed into the $L1_2$ cubic structure

Table 3. Characteristics of trialuminides synthesized in the $x(TiH_2)–(1 - x)\ (ZrH_2)–3Al$ system ($TiAl_3–ZrAl_3$ section)

Starting reagents, at %			Phase composition; crystal lattice; parameters, Å; c/a	Formula	Density, g/cm^3	
TiH_2	ZrH_2	Al			hydro-stat.	X-ray
0	25	75	Tetragonal $ZrAl_3 - I_{4/mmm}$; BCT ($D0_{23}$); $a = 4.015$, $c = 17.318$, 4.313	$Zr_{0.25}Al_{0.75}$	3.863	4.09
5	20	75	Tetragonal, based on $ZrAl_3$; $a = 3.992$, $c = 17.189$; 4.306	$Ti_{0.05}Zr_{0.2}Al_{0.75}$	3.075	3.617
10	15	75	Tetragonal, based on $ZrAl_3$; $a = 3.979$, $c = 17.211$; 4.325	$Ti_{0.1}Zr_{0.15}Al_{0.75}$	2.939	3.444
12.5	12.5	75	Tetragonal, based on $ZrAl_3$; $a = 3.953$, $c = 17.063$; 4.316	$Ti_{0.125}Zr_{0.125}Al_{0.75}$	2.729	3.368
15	10	75	Tetragonal, based on $ZrAl_3$ and $TiAl_3$ traces; $a = 3.95$, $c = 16.947$; 4.29	$Ti_{0.15}Zr_{0.1}Al_{0.75}$	2.603	3.351
20	5	75	Tetragonal $TiAl_3$; $a = 3.852$, $c = 8.633$; 2.241; tetragonal $ZrAl_3$; $a = 3.937$, $c = 16.849$; 4.279	$Ti_{0.2}Zr_{0.05}Al_{0.75}$	2.617	–
25	0	75	Tetragonal $TiAl_3 - I_{4/mmm}$(139), BCT ($D0_{22}$); $a = 3.856$, $c = 8.648$; 2.242	$Ti_{0.25}Al_{0.75}$	2.564	3.326

by doping it with Period 4 transition elements such as Cr, Mn, Fe, Co, Ni, Cu, and Zn or Group 4 elements Ti, Zr, and Hf [5–7]. Arc melting is a common method for the synthesis of titanium and zirconium trialuminides [5]; as a result, when the temperature is raised from 1408 to 1607°C, the $TiAl_3–ZrAl_3$ phases are mainly formed. According to [5, 6], aluminides $Al_3(Ti_xZr_{1-x})$ with an fcc lattice of $L1_2$ type or tetragonal structure ($D0_{22}$ or $D0_{23}$) form in the Al–Ti–Zr ternary systems depending on the composition and synthesis conditions. Limited solid solutions of compounds based on $TiAl_3$ and $ZrAl_3$ (in the $TiAl_3–ZrAl_3$ section) were detected [6]. Titanium and zirconium aluminides were also obtained by metal dissolution in an aluminum melt at temperatures below 800°C [7, 22]. The structure of the $D0_{22}$ ($TiAl_3$) type dissolves up to 2 at % Zr, while the structure of the $D0_{23}$ ($ZrAl_3$) type exists in a wide range of compositions: from pure $ZrAl_3$ to ≈15 at % Ti [5, 22].

We synthesized single-phase $TiAl_3$ and $ZrAl_3$ by the HC method [13, 15]. This section presents the results of our studies of the formation of titanium and zirconium trialuminides in the HC mode: $(TiH_2)_x + (ZrH_2)_{1-x} + 3Al \rightarrow (Ti_xZr_{1-x})Al_3 + H_2\uparrow$, $0 \le x \le 1$.

The formulas and characteristics of the synthesized trialuminides are presented in Table 3. The characteristics of binary aluminides $ZrAl_3$ and $TiAl_3$ are also given there for comparison. According to Table 3, single- and double-phase trialuminides were obtained in the HC mode. It was shown that the changes in the parameters of the HC process, press force from 20000 to 45000 kgf, process temperature from 900 to 1000°C, and heating rate from 20 to 40°C/min do not significantly affect the phase composition of the synthesized trialuminides. Similar results were obtained in the synthesis of $ZrAl_3$, $TiAl_3$, $NbAl_3$, and $Ti_xNb_{1-x}Al_3$.

As the temperature increased, the exo effects were observed at 660–670°C on the thermograms. Similar exo effects were recorded for all compositions of this system under study and for previously studied binary trialuminides $TiAl_3$, $NbAl_3$, and $ZrAl_3$ [6–8].

Figure 2 shows the diffraction patterns of single-phase ((a) $Ti_{0.1}Zr_{0.15}Al_{0.75}$) and double-phase ((b) $Ti_{0.2}Zr_{0.05}Al_{0.75}$) aluminides. At 1–15 at % TiH_2 in the batch (lines 1–4 in Table 3), single-phase trialuminides with a tetragonal $D0_{23}$ crystal structure (close to that of $ZrAl_3$, Fig. 2a) formed. At 15 at % TiH_2 (line 4 in Table 3), traces of the $TiAl_3$ phase appeared in the diffraction patterns. When the TiH_2 concentration reached 20 at % (lines 5 and 6, Table 3), the double-phase aluminide $Ti_{0.2}Zr_{0.05}Al_{0.75}$ containing the $TiAl_3$ ($D0_{22}$) and $ZrAl_3$ ($D0_{23}$) phases formed (Fig. 6b). These data of Table 3 (lines 5 and 6) are consistent with the conclusion of the authors of [5] about the limited mutual solubility of $TiAl_3$ and $ZrAl_3$.

Figure 3 shows the DTA curves recorded for trialuminides and previously obtained Ti and Zr hydrides [13, 15]: (a) TiH_2, (b) TiH_2 + 3Al, (c) ZrH_2, (d) ZrH_2 +

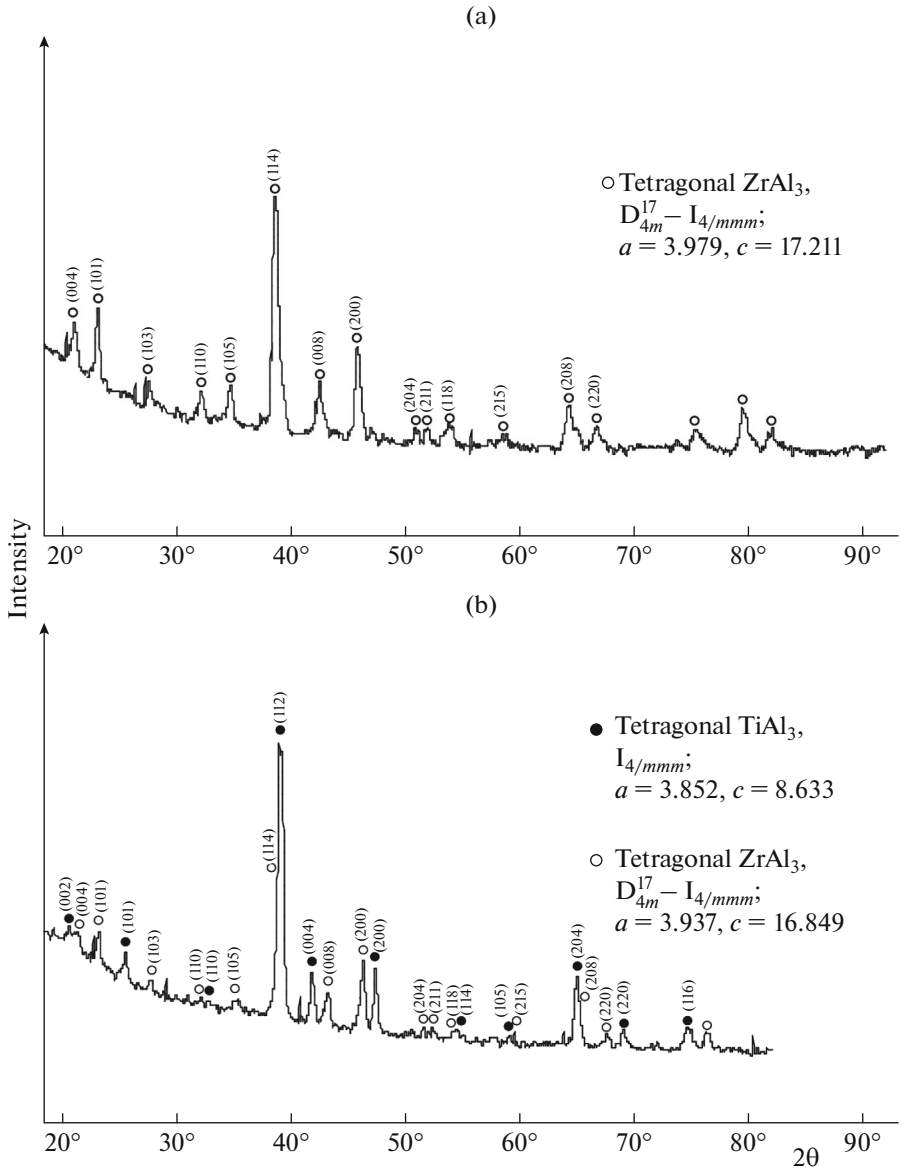

Fig. 2. Diffraction patterns of aluminides (a) $Ti_{0.1}Zr_{0.15}Al_{0.75}$ and (b) $Ti_{0.2}Zr_{0.05}Al_{0.75}$.

3Al, (e) $0.8TiH_2 + 0.2ZrH_2 + 3Al$, and (f) $0.2TiH_2 + 0.8ZrH_2 + 3Al$. Two endo effects were observed on the DTA curves during the decomposition of titanium hydride: at 540 and 640°C (Fig. 3a). An exo effect appeared at 680°C on the DTA curve for the $TiH_2 + 3Al$ mixture, due to the interaction of released Ti with Al, in addition to the two endo effects characteristic of TiH_2 dissociation (Fig. 3b). Three endo effects were recorded on the DTA curve during the dissociation of zirconium hydride: at 150, 460, and 840°C (Fig. 3c). The DTA curve for the $ZrH_2 + 3Al$ mixture shows one endo effect due to the decomposition of ZrH_2 at 550°C to the fcc structure of $ZrH_{1.5}$ and the subsequent exo effect at 670°C, indicating that $ZrH_{1.5}$ reacted with Al, forming zirconium trialuminide (Fig. 3d). The exo effects recorded on DTA curves *2* for the mixtures $0.8TiH_2 + 0.2ZrH_2 + 3Al$ (Fig. 3e) and $0.2TiH_2 + 0.8ZrH_2 + 3Al$ (Fig. 3f) coincide with the temperatures of the start of the exo effects observed on the HC thermograms. The results of quenching of the intermediate products of the reactions both in HC and DTA and at 670°C followed by phase analysis confirmed the formation of trialuminides.

RESULTS AND DISCUSSION

Table 4 shows the values of the thermal effects that accompany the formation of binary and ternary aluminides based on titanium and zirconium both during HC and thermal analysis (DTA).

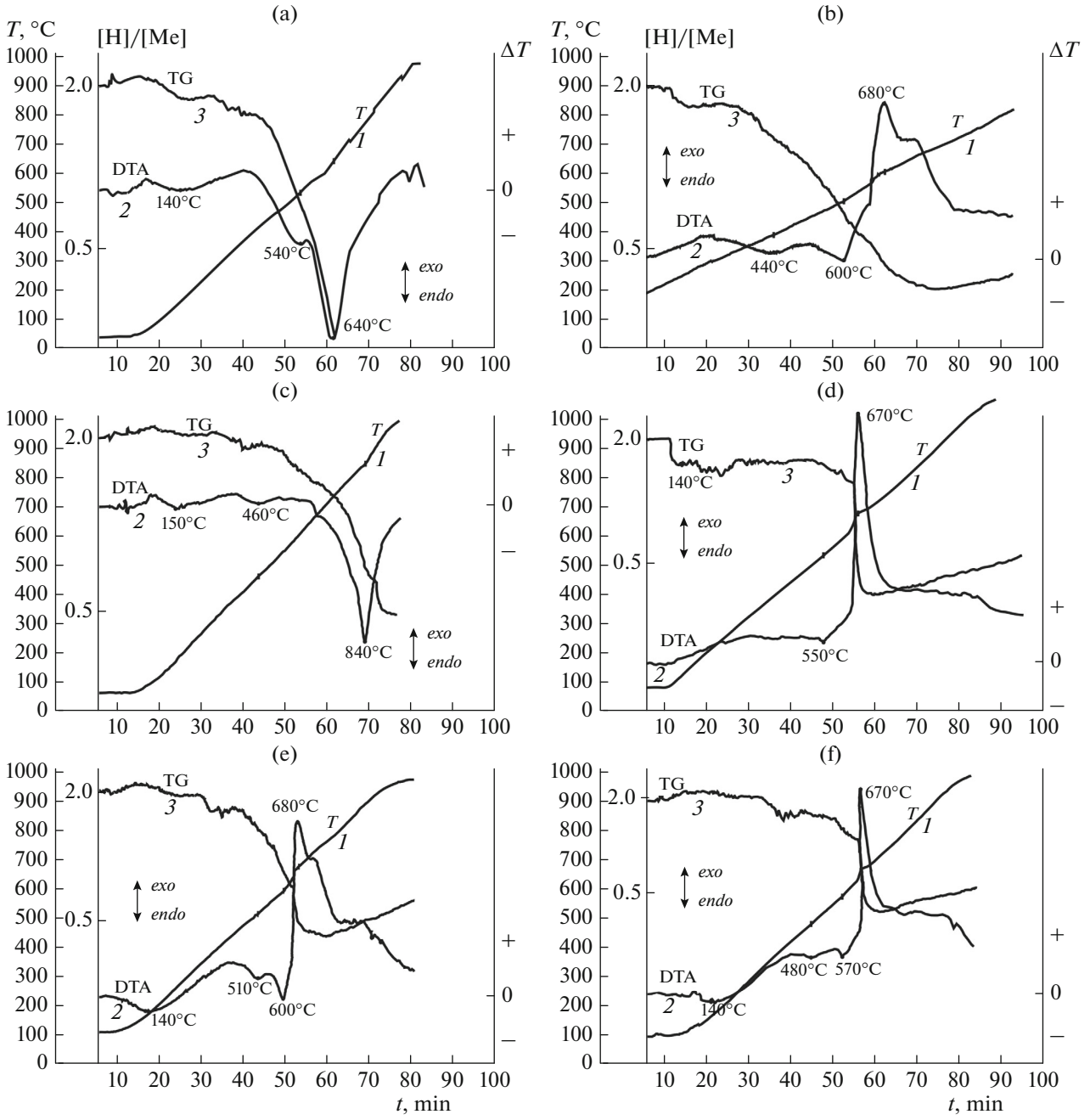

Fig. 3. DTA curves for hydrides and mixtures: (a) TiH_2, (b) TiH_2 + 3Al, (c) ZrH_2, (d) ZrH + 3Al, (e) $0.8TiH_2 + 0.2ZrH_2$ + 3Al ($Ti_{0.2}Zr_{0.05}Al_{0.75}$), and (f) $0.2TiH_2 + 0.8ZrH_2$ + 3Al ($Ti_{0.05}Zr_{0.2}Al_{0.75}$).

Analyzing the data of Table 4, we can say with confidence that the formation of binary and multicomponent aluminides during HC and DTA starts with an exothermal reaction at $T = 650–670$°C at any aluminum content (25, 50, and 75 at %). It is assumed that an aluminum-rich layer (of the $MeAl_3$ type) initially forms on the surface of metal grains; therefore, the temperature of the exo effects is always within the range of $T = 650–670$°C for all aluminum compounds (25, 50, 75 at %). Subsequently, homogenization (or diffusion of aluminum inside the grain) occurs when the heating temperature increases to 1000°C and this temperature is maintained for 30–60 min for compositions with 25 and 50 at % Al, leading to the formation of a definite phase. For the aluminum-rich samples (75 at % Al), the formation of trialuminides ($TiAl_3$, $ZrAl_3$, $Ti_{0.2}Zr_{0.05}Al_{0.75}$, and $Ti_{0.05}Zr_{0.2}Al_{0.75}$) occurs at 650–670°C, as confirmed by the XRD analysis of the quenched products of HC and DTA.

Table 4. Temperatures of endo and exo effects observed during the formation of aluminides in HC and during DTA

Thermal effects	$Me(M')_3Al$			
	α_2-Ti_3Al, $Ti_{0.75}Al_{0.25}$	Zr_3Al ($Zr_{0.75}Al_{0.25}$)	$Ti_{0.55}Al_{0.25}Zr_{0.2}$	$Ti_{0.25}Al_{0.25}Zr_{0.5}$
Temperatures of the start of exo effects in °C from the thermograms of HC				
Exo effect	660	670	670	660
Temperatures of thermal effects from the DTA curves				
Exo effect	670	630	670	650
Endo effect	480, 600	150, 550, 790	150, 520, 640, 820	150, 480, 570, 780
Thermal effects	Me(M')Al			
	γ-TiAl	ZrAl	$Ti_{0.4}Zr_{0.1}Al_{0.5}$	$Ti_{0.45}Zr_{0.05}Al_{0.5}$
Temperatures of the start of exo effects in °C from the thermograms of HC				
Exo effect	650	650	670	660
Temperatures of thermal effects from the DTA curves in °C				
Exo effect	670	670	670	680
Endo effect	530, 630	150, 520, 800	150, 500, 600, 740	150, 510, 620, 730
Thermal effects	$Me(M')Al_3$			
	$TiAl_3$	$ZrAl_3$	$Ti_{0.2}Zr_{0.05}Al_{0.75}$	$Ti_{0.05}Zr_{0.2}Al_{0.75}$
Temperatures of the start of exo effects (°C) from the thermograms of HC				
Exo effect	650	650	670	660
Temperatures of thermal effects from the DTA curves (°C)				
Exo effect	680	670	680	670
Endo effect	440, 600	550	140, 510, 600, 720	140,480, 570, 780

Based on the results of our study, we can describe the following mechanism of the formation of aluminides based on titanium and zirconium. During the heating of the batch $xTiH_2 + yZrH_2 + zAl \rightarrow Ti_xAl_zZr_y$ at $T = 600–1000$°C in the HC, the starting hydrides decompose, and the Me–H bonds are destroyed, leading to strong activation of titanium and zirconium and their instantaneous exothermal interaction with aluminum, skipping the aluminum melting stage. The thermograms of all the composites under study did not show any endo effects associated with the decomposition of the starting hydrides, although they surely did occur. Also, there were no traces of melting on the synthesized samples. Thus, the formation of all the titanium and zirconium aluminide phases under study proceeds by the solid-phase mechanism. Similar examples of the solid-phase mechanism of formation of alloys and intermetallic compounds based on refractory metals, skipping the melting stage of the starting reagents, were reported in our previous studies [9–16].

A concentration triangle of the Ti–Al–Zr system was constructed (Fig. 4) based on the results obtained in the study of the formation of titanium and zirconium aluminides of the systems given below, with titanium aluminides (Ti–Al) [13], zirconium aluminides (Zr–Al) [15], and previously studied alloys based on Ti–Zr synthesized by the HC method [9] shown on its sides. The positions of the single-, double-, and triple-phase aluminides based on titanium and zirconium are shown inside the triangle.

The Ti_3Al–Zr_3Al section (25 at. % Al) shows the phase composition of the following aluminides (Fig. 4): **1**—$Ti_{0.65}Al_{0.25}Zr_{0.1}$($DO_{19}$ + B_2); **2**—$Ti_{0.55}Al_{0.25}Zr_{0.2}$($B_2$ + $D0_{19}$); **3**—$Ti_{0.45}Al_{0.25}Zr_{0.3}$($B_2$ + $D0_{19}$); **4**—$Ti_{0.35}Al_{0.25}Zr_{0.4}$($B_2$ + sol. soln. of Al and Ti in Zr); **5**—$Ti_{0.25}Al_{0.25}Zr_{0.5}$ (sol. soln. of Al and Ti in Zr + B_2); **6**—$Ti_{0.15}Al_{0.25}Zr_{0.6}$ (sol. soln. of Al and Ti in Zr + B_2).

The TiAl–ZrAl section (50 at. % Al) shows the phase composition of the following aluminides (Fig. 4): **7**—$Ti_{0.5}Al_{0.48}Zr_{0.02}$(γ-TiAl + X phase); **8**—$Ti_{0.47}Al_{0.47}Zr_{0.06}$ (γ-TiAl + Al_2Zr); **9**—$Ti_{0.4}Al_{0.5}Zr_{0.1}$(γ-TiAl + Al_2Zr); **10**—$Ti_{0.3}Al_{0.5}Zr_{0.2}$(Al_2Zr + γ-TiAl); **11**—$Ti_{0.25}Al_{0.5}Zr_{0.25}$ (Al_2Zr + γ-TiAl); **12**—$Ti_{0.2}Al_{0.5}Zr_{0.3}$(Al_2Zr + γ-TiAl); **13**—$Ti_{0.1}Al_{0.5}Zr_{0.4}$; **14**—$Ti_{0.5}Al_{0.4}Zr_{0.1}$(γ-TiAl + $ZrAl_2$);

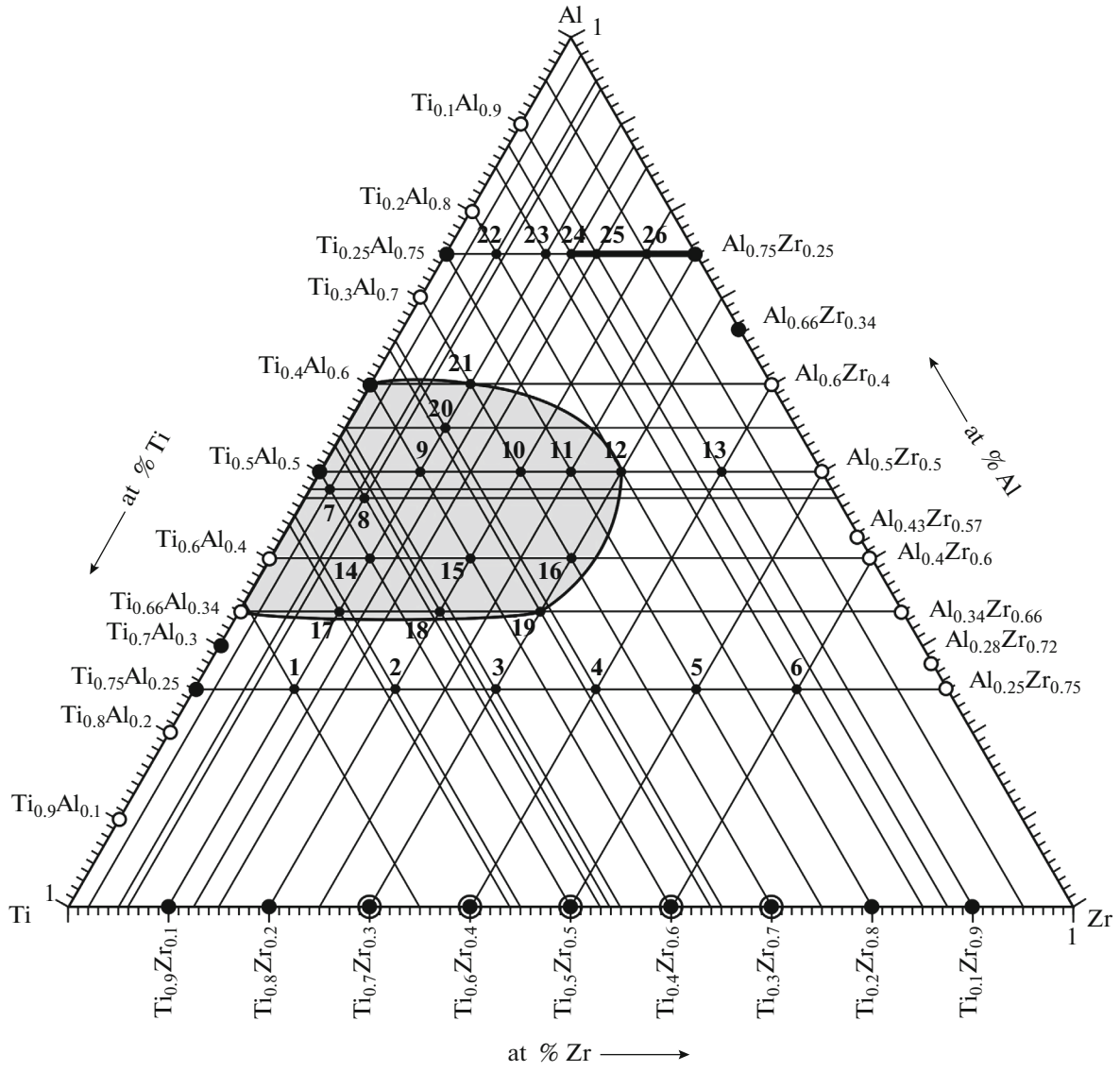

Fig. 4. Concentration triangle of the Ti–Al–Zr system.

15—$Ti_{0.4}Al_{0.4}Zr_{0.2}$(γ-TiAl + $ZrAl_2$); **16**—$Ti_{0.3}Al_{0.4}Zr_{0.3}$; ($ZrAl_2$ + γ-TiAl); **17**—$Ti_{0.56}Al_{0.34}Zr_{0.1}$(γ-TiAl + $ZrAl_2$); **18**—$Ti_{0.46}Al_{0.34}Zr_{0.2}$(γ-TiAl + $ZrAl_2$); **19**—$Ti_{0.36}Al_{0.34}Zr_{0.3}$ (γ-TiAl + $ZrAl_2$); **20**—$Ti_{0.35}Al_{0.55}Zr_{0.1}$(γ-TiAl + $ZrAl_2$); **21**—$Ti_{0.3}Al_{0.6}Zr_{0.1}$(γ-TiAl + $ZrAl_2$).

The γ-TiAl and hexagonal $ZrAl_2$ phases formed in different ratios depending on the composition of the starting mixture. Inside the concentration triangle, the region of two-phase aluminides of various compositions around the γ-TiAl binary phase was isolated (structure $L1_0$).

The $TiAl_3$–$ZrAl_3$ section (75 at. % Al) shows the following single- and double-phase trialuminides (Table 3, Fig. 4): **22**—$Ti_{0.2}Al_{0.75}Zr_{0.05}$($TiAl_3$ + $ZrAl_3$); **23**—$Ti_{0.15}Al_{0.75}Zr_{0.1}$($ZrAl_3$ + $TiAl_3$ traces); **24**—$Ti_{0.125}Al_{0.75}Zr_{0.125}$($ZrAl_3$); **25**—$Ti_{0.1}Al_{0.75}Zr_{0.15}$($ZrAl_3$); **26**—$Ti_{0.05}Al_{0.75}Zr_{0.2}$($ZrAl_3$).

CONCLUSIONS

(1) A series of single- and double-phase aluminides based on titanium and zirconium were synthesized (Tables 1–3): sol. soln. of Ti and Al in the Zr hcp; B_2 and (α_2) DO_{19} phases; a series of alloys based on Ti, Al, and Zr of various compositions around the γ-TiAl ($L1_0$) binary phase; single-phase trialuminides with a tetragonal structure based on $ZrAl_3$ ($Ti_{0.05}Zr_{0.2}Al_{0.75}$, $Ti_{0.1}Zr_{0.15}Al_{0.75}$, $Ti_{0.125}Zr_{0.125}Al_{0.75}$).

(2) It was shown that the ratio of the starting components of the batch, the temperature, and heating

rate of the initial mixture have the greatest effect on the formation of aluminides in the HC mode.

(3) During the synthesis of aluminides in the TiH_2–ZrH_2–Al system in the HC mode, the metals are strongly activated due to the destruction of the Me–H bond and removed from the oxide film. The "open bonds," cleaned surface of the activated titanium and zirconium powders, and nanosized crystallite particles (20–80 nm) of the powders used create favorable conditions for the solid-phase diffusion mechanism for the formation of aluminides, skipping the melting stage of the initial components.

(4) It was shown that some of the synthesized aluminides without pre-crushing interact with hydrogen in the SHS mode with formation of reversible hydrides.

(5) The concentration triangle of the Ti–Al–Zr system was constructed, inside of which the positions of the ternary aluminide phases are shown for 26 composites containing B_2 + $D0_{19}$, γ-TiAl, etc.

(6) The synthesis of aluminides based on titanium and zirconium in HC has significant advantages over the existing methods: relatively low temperatures (~1000°C) and process time (30–60 min), formation of single-phase aluminides in one technological stage. The aluminides $Ti_{0.25}Al_{0.75}$, $Zr_{0.25}Al_{0.75}$, $Ti_{0.2}Zr_{0.05}Al_{0.75}$, $Ti_{0.05}Zr_{0.2}Al_{0.75}$, and other composites are synthesized at relatively low temperatures (650–670°C).

REFERENCES

1. L. Tretyachenko, in *Light Metal Systems. Al–Ti–Zr (Aluminium–Titanium–Zirconium),* Ed. by G. Effenberg and S. V. Ilyenko, Vol. 11A4 of *Landolt-Börnstein–Group IV Physical Chemistry* (Springer, Heidelberg, 2005), p. 54.
2. Kai-li Lu, Feng Yang, Zhi-yun Xie, et al., Trans. Nonferr. Met. Soc. China **26**, 3052 (2016).
3. D. Tanda, T. Tanabe, R. Tamura, et al., Mater. Sci. Eng. **387**, 991 (2004).
4. Y. Miyajima, K. Ishikawa, and K. Aoki, Mater. Trans. **43**, 1085 (2002).
5. K. E. Knipling, D. C. Dunand, and D. N. Seidman, Acta Mater. **56**, 1182 (2008).
6. M. V. Karpets, Yu. V. Milman, O. M. Barabash, et al., Intermetallics **11**, 241 (2003).
7. O. Dezellus, B. Gardiola, and J. Andrieux, J. Phase Equilib. Difus. **35**, 120 (2014).
8. G. J. Fan, X. P. Song, M. X. Quan, et al., Mater. Sci. Eng., A, No. 231, 111 (1997).
9. S. K. Dolukhanyan, A. G. Aleksanyan, O. P. Ter-Galstyan, V. Sh. Shekhtman, M. K. Sakharov, and G. E. Abrosimova, Russ. J. Phys. Chem. B **1**, 563 (2007).
10. H. G. Hakobyan, A. G. Aleksanyan, S. K. Dolukhanyan, et al., Int. J. SHS **19**, 49 (2010).
11. A. G. Aleksanyan, S. K. Dolukhanyan, V. Sh. Shekhtman, et al., J. Alloys Compd. **509**, 786 (2011).
12. A. G. Aleksanyan, S. K. Dolukhanyan, V. Sh. Shekhtman, et al., Int. J. Hydrogen Energy **37**, 14234 (2012).
13. S. K. Dolukhanyan, A. G. Aleksanyan, O. P. Ter-Galstyan, et al., Int. J. Self-Propag. High-Temp Synth. **23**, 78 (2014).
14. S. K. Dolukhanyan, O. P. Ter-Galstyan, A. G. Aleksanyan, A. G. Hakobyan, N. L. Mnatsakanyan, and V. Sh. Shekhtman, Russ. J. Phys. Chem. B **9**, 702 (2015).
15. G. N. Muradyan, Arm. Khim. Zh. **69**, 416 (2016).
16. S. K. Dolukhanyan, O. P. Ter-Galstyan, A. G. Aleksanyan, G. N. Muradyan, and N. L. Mnatsakanyan, Russ. J. Phys. Chem. B **11**, 272 (2017).
17. S. K. Dolukhanyan, in *Self-Propagating High-Temperature Synthesis of Materials,* Ed. by A. A. Borisov, L. de Luca, and A. G. Merzhanov, Vol. 5 of *Combustion Science and Technology Book Series* (Taylor Francis, New York, 2002), p. 219.
18. V. Sh. Shekhtman, S. K. Dolukhanyan, A. G. Aleksanyan, et al., Int. J. Hydrogen Energy **26**, 435 (2001).
19. C. Ravi and R. Asokamani, Bull. Mater. Sci. **26**, 97 (2003).
20. X. F. Chen, R. D. Reviere, B. F. Oliver, et al., Scr. Met. Mater. **27**, 45 (1992).
21. R. Kainuma, Y. Fujita, H. Mitsui, et al., Intermetallics **8**, 855 (2000).
22. E. A. Popova, A. B. Shubin, P. V. Kotenkov, E. A. Pastukhov, L. E. Bodrova, and O. M. Fedorova, Russ. Metall. **2012**, 357 (2012).

Translated by L. Smolina